

IQGAP1 Stimulates Proliferation and Enhances Tumorigenesis of Human Breast Epithelial Cells*

Received for publication, October 11, 2007 Published, JBC Papers in Press, November 2, 2007, DOI 10.1074/jbc.M708466200

Lorraine Jadeski^{‡§1}, Jennifer M. Mataraza^{‡1,2}, Ha-Won Jeong[‡], Zhigang Li[‡], and David B. Sacks^{‡3}

From the [‡]Department of Pathology, Brigham and Women's Hospital and Harvard Medical School, Boston, Massachusetts 02115 and the [§]Department of Human Biology and Nutritional Sciences, University of Guelph, Guelph, Ontario N1G 2W1, Canada

The scaffold protein IQGAP1 integrates signaling pathways and participates in diverse cellular activities. IQGAP1 is overexpressed in a number of human solid neoplasms, but its functional role in tumorigenesis has not been previously evaluated. Here we report that IQGAP1 contributes to neoplastic transformation of human breast epithelial cells. The amount of IQGAP1 in breast carcinoma is greater than that in normal tissue, with highly metastatic breast epithelial cells expressing the highest levels. Overexpression of IQGAP1 enhances proliferation of MCF-7 breast epithelial cells. Reduction of endogenous IQGAP1 by RNA interference impairs both serum-dependent and anchorage-independent growth of MCF-7 cells. Consistent with these *in vitro* observations, immortalized MCF-7 cells overexpressing IQGAP1 form invasive tumors in immunocompromised mice, whereas tumors derived from MCF-7 cells with stable knockdown of IQGAP1 are smaller and less invasive. *In vitro* analysis with selected IQGAP1 mutant constructs and a chemical inhibitor suggests that actin, Cdc42/Rac1, and the mitogen-activated protein kinase pathway contribute to the mechanism by which IQGAP1 increases cell invasion. Collectively, our data reveal that IQGAP1 enhances mammary tumorigenesis, suggesting that it may be a target for therapeutic intervention.

Tumor progression that culminates in clinically relevant metastatic lesions is the end point of a complex sequence of interrelated cellular events. After the initial transforming event, tumor cell proliferation, invasion, and migration, as well as vascularization of the tumor mass, occur. A thorough understanding of the molecular mechanisms that regulate tumor progression will provide the biological foundation for improving the efficacy of current therapeutic interventions (1–3).

IQGAP1 is a 189-kDa scaffolding protein that contains multiple protein-interacting domains (for reviews see Refs. 4–7). These include a calponin homology domain, a polyproline-binding domain, four calmodulin-binding motifs, and a RasGAP-related domain. The motifs present in IQGAP1 are

involved in the interaction of IQGAP1 with specific proteins, such as actin, calmodulin, members of the Rho GTPase family (*i.e.* Rac1 and Cdc42), Rap1, E-cadherin, β -catenin, members of the mitogen-activated protein kinase (MAPK)⁴ pathway, and adenomatous polyposis coli (7, 8). By interacting with these proteins, IQGAP1 regulates multiple fundamental cellular activities including cytoskeletal organization, cell-cell adhesion, cell migration, transcription, and signal transduction. For example, binding of IQGAP1 to β -catenin both disrupts the E-cadherin-catenin complex, inhibiting epithelial cell-cell adhesion (9), and increases β -catenin-mediated transcriptional activation (10). IQGAP1 increases active Cdc42 in mammalian cells, resulting in formation of actin filopodia and microspikes (11), and promotion of cell migration and invasion (12). These morphological and functional changes are not observed with a mutant IQGAP1 construct with impeded Cdc42-mediated signaling (11, 12). More recently, functional significance of IQGAP1 in MAPK signaling was demonstrated; IQGAP1 modulates epidermal growth factor-mediated activation of extracellular signal-regulated kinase (ERK) and MAPK/ERK kinase (MEK) (13, 14). In addition, IQGAP1 is required for epidermal growth factor to increase B-Raf activity (15). These findings suggest that IQGAP1 serves as a scaffolding protein that mediates multiprotein complex assembly and participates in cytoskeletal activation and coordination of signaling (5, 7).

Accumulating evidence implicates IQGAP1 in tumorigenesis and tumor progression. Many of the identified IQGAP1-binding partners contribute to malignant transformation and/or tumor progression, and several cellular functions effected as a consequence of IQGAP1 binding are important in tumor biology (5, 7). Furthermore, genomic studies suggest IQGAP1 involvement in tumorigenesis; the IQGAP1 gene is amplified in diffuse gastric cancer cell lines (16) and is up-regulated in lung (17) and colon (18) carcinoma relative to noncancerous control tissue. At the post-transcriptional level, IQGAP1 mRNA was increased in an oligonucleotide array screen of gene expression in melanoma-derived pulmonary metastases compared with that in poorly metastatic tumor cells (19). Protein analyses substantiate involvement of IQGAP1 in tumorigenesis. For example, IQGAP1 protein is overexpressed

* This work was supported in part by a grant from the National Institutes of Health (to D. B. S.). The costs of publication of this article were defrayed in part by the payment of page charges. This article must therefore be hereby marked "advertisement" in accordance with 18 U.S.C. Section 1734 solely to indicate this fact.

¹ These authors contributed equally to this work.

² Present address: Organon Research Center, Cambridge, MA 02142.

³ To whom correspondence should be addressed: Brigham and Women's Hospital, Thorn 530, 75 Francis St. Boston, MA 02115. Tel.: 617-732-6627; Fax: 617-278-6921; E-mail: dsacks@rics.bwh.harvard.edu.

⁴ The abbreviations used are: MAPK, mitogen-activated protein kinase; ERK, extracellular signal-regulated kinase; MEK, MAPK/ERK kinase; DMEM, Dulbecco's modified Eagle's medium; WASP, Wiskott Aldrich syndrome protein; GBD, GTPase-binding domain; PAK, p21-activated kinase; CRIB, Cdc42-Rac1-interactive binding domain; MTT, 3-[4,5-dimethylthiazol-2-yl]-2,5-diphenyl tetrazolium bromide; GST, glutathione S-transferase; FBS, fetal bovine serum.

in several human neoplasms, including gastric (16), colorectal (20), lung (21), ovary (22), and liver (23). In addition, the subcellular location of IQGAP1 is altered in neoplasia. The IQGAP1 overexpression in colorectal carcinoma is most apparent at the invasive front and in advanced carcinomas with the highest invasive potential (20). Similarly, immunohistochemical analyses of gastric carcinomas suggest that subcellular location of IQGAP1 varies depending on the degree of differentiation of the tumor. In poorly and well differentiated diffuse- and intestinal-type tumors, IQGAP1 is localized at the cell membrane and in the cytoplasm, respectively (24). The localization of IQGAP1 has recently been shown to have prognostic information. In ovarian carcinoma, overexpression and a diffuse expression pattern of IQGAP1 were shown to be independent predictors of highly aggressive tumors (22).

The relevance to tumor biology of the known cellular targets of IQGAP1, combined with accumulating clinical and experimental evidence, suggest a positive relationship between IQGAP1 expression and tumorigenesis. Notwithstanding these data, it is not known whether the changes in IQGAP1 observed in these studies contribute to the tumor pathogenesis nor whether the alterations in IQGAP1 are a cause or consequence of the neoplastic transformation. To investigate these issues, we chose to directly examine the role of IQGAP1 in tumorigenesis. Analysis was performed with cultured cells *in vitro* and with an *in vivo* tumor model system. Female immunocompromised mice (*i.e.* NOD.CB17-Prkdc^{scid}/JCH/HeJ) were injected subcutaneously with one of three MCF-7-derived cell lines, which express varying amounts of IQGAP1. Differences between groups in *in vitro* and *in vivo* proliferation and tumorigenic growth were monitored.

EXPERIMENTAL PROCEDURES

Plasmids—Myc-tagged wild type human IQGAP1 in a pcDNA3 vector was used (25, 26). The construction of IQGAP1ΔGRD, IQGAP1G75Q and IQGAP1ΔMK24 has been described previously (27–29). Myc-tagged forms of the dominant negative constructs N17Cdc42 and N17Rac1 (30) were kindly provided by Alan Hall (University College London).

Preparation of Fusion Proteins—GST-WASP-GBD (glutathione S-transferase Wiskott Aldrich Syndrome protein GTPase-binding domain) and GST-PAK-CRIB (p21-activated kinase Cdc42-Rac1-interactive binding domain) were expressed in *Escherichia coli* and isolated with glutathione-Sepharose as previously described (12, 26, 31).

Cell Culture and Transfection—The following human breast epithelial cell lines were used: T47D, ZR-75-1, MDA-MB-231, MDA-MB-361 (generously provided by Andrea Richardson, Brigham and Women's Hospital), MCF-7, Hs578T, and MDA-MB-435s (purchased from ATCC). The cells were cultured and transfected essentially as previously described (11, 32). Briefly, the cells were grown in Dulbecco's modified Eagle's medium (DMEM) supplemented with 10% (v/v) fetal bovine serum. Where indicated, the cells were transiently transfected with 10 μg of pcDNA3 (empty vector), Myc-IQGAP1, Myc-IQGAP1ΔGRD, Myc-IQGAP1G75Q, or Myc-IQGAP1ΔMK24 using FuGENE 6. In addition, MCF-7 human breast epithelial cells were stably transfected with empty pcDNA3 vector

(MCF/V) or pcDNA3-Myc-IQGAP1 (MCF/I); IQGAP1 protein expression is 3-fold higher in MCF/I relative to MCF/V cells (10, 11). Stable knockdown of IQGAP1 was obtained by integrating into the genome of MCF-7 cells, a specific siRNA targeted against IQGAP1 (12). IQGAP1 protein expression in these cells (termed MCF-siIQ8 cells) is reduced by 80% (12).

Western Blotting—The cells were washed three times in serum-free medium and lysed in buffer A (50 mM Tris, pH 7.4, 140 mM NaCl, and 1% (v/v) Triton X-100). Equal amounts of protein lysate were resolved by SDS-PAGE and transferred to polyvinylidene difluoride membrane essentially as previously described (33–35). Immunoblots were probed with anti-IQGAP1 monoclonal antibody and anti-tubulin antibody (Sigma). The complexes were visualized with horseradish peroxidase-conjugated secondary antibody and developed by ECL. Frozen human breast tissue was thawed and homogenized in buffer A containing 1 mM EGTA and protease inhibitors. Equal amounts of protein were resolved by Western blotting.

Animals—Female NOD.CB17-Prkdc^{scid}/JCH/HeJ mice (6–8 weeks old) were obtained from Jackson Laboratory (Bar Harbor, ME). Upon arrival at the vivarium, the animals were immediately randomized to treatment groups (*i.e.* MCF/V, MCF/I, and MCF-siIQ8 cell lines). The experimental procedures began after a 1-week acclimatization period. Throughout the investigation, the animals had free access to food (standard mouse chow) and water and were maintained on a 12-h light/dark cycle. The mice were housed in cages fitted with a high efficiency particulate air filter lid; the cages were contained in a chamber receiving independent, filtered air. All of the manipulations on mice were performed in a laminar flow hood using sterile procedures. The cages, bedding, food, water, nestlets, and water bottles were autoclaved prior to contact with mice. The water was acidified or supplemented with antibiotics on a rotating 4-day schedule. The animals were treated in accordance with guidelines set out by the Canadian Council on Animal Care.

Cell Proliferation Assays—Incorporation of [³H]thymidine and the 3-[4,5-dimethylthiazol-2-yl]-2,5-diphenyl tetrazolium bromide (MTT) dye method were used to assess cell proliferation. The cells were made quiescent by culturing them for 24 h in DMEM containing 0.5% (v/v) FBS. DNA synthesis was measured by labeling 2 × 10⁵ cells with 1 μCi/ml [³H]thymidine for 18 h. The cells were washed with ice-cold 0.5% trichloroacetic acid and lysed with 0.25 M NaOH. Six hundred microliters of lysate was collected, and radioactivity assessed by liquid scintillation spectrometry. All of the assays were performed in quadruplicate. For the MTT assay, MCF/V and MCF/I cells were transfected with 1 μg of empty pcDNA vector, N17Cdc42, or N17Rac1. After 36 h, 5 × 10³ viable cells were plated in 96-well, flat-bottom tissue culture plates. After incubating for 24, 48, and 72 h at 37 °C in 5% CO₂, 20 μl of MTT labeling reagent was added, and the cells were incubated for another 4 h. Dimethyl sulfoxide (100 μl) was added to each well, and the samples were incubated overnight. The absorbances were determined at 550 nm using a Victor3 Multilabel Counter (PerkinElmer Life Sciences).

Soft Agar Colony Formation Assay—Colony growth assays were performed essentially as previously described (36, 37).

Briefly, a 5-ml agar solution (0.6% Difco agar in DMEM supplemented with 10% FBS) was layered onto 15-mm tissue culture plates. The cells (1×10^4 ; MCF/V, MCF/I and MCF-silQ8) were then suspended in soft agar (0.36% Bactoagar solution in DMEM) and layered onto prepared 0.6% Difco agar plates. After a 14-day incubation at 37 °C in 5% CO₂, colonies (>0.2 mm) were counted using a light microscope. All of the assays were performed in quadruplicate.

In Vivo Assay for Primary Tumor Growth and Angiogenesis—The mice were anesthetized using an intraperitoneal injection of a hypnorm/midazolam mixture. Specifically, 1 part hypnorm (fentanyl citrate, 0.315 mg; fluanison, 10 mg/ml) and 1 part midazolam (5 mg/ml) were suspended in 2 parts of sterile water; the dose was 0.1 ml/10 g of body weight. Incision sites were cleaned using a three-step surgical preparation: isopropyl alcohol, tincture of iodine, and savlon. Hypromellose eye lubricant prevented ocular drying and damage during anesthesia. In the inguinal region, the mice received subcutaneous implants of 1×10^5 tumor cells (*i.e.* MCF/V, MCF/I, or MCF-silQ8; 10 animals/group) suspended in Matrigel (Collaborative Research, Bedford, MA) (3.5 mg of Matrigel in 0.5 ml of DMEM), and on the contralateral side as controls, they received the equivalent amount of Matrigel alone. A small incision was made in the dorsal scapular region, and a slow release (60 day) 17 β -estradiol pellet (Innovative Research of America, Sarasota, FL) was inserted subcutaneously. The incisions were then closed using a small drop of Vetbond surgical glue. During recovery from anesthesia, the mice were placed in a warm cage; they were monitored carefully and received subcutaneous injections of warmed saline (0.9%; 1 ml).

As an indication of general health, the mice were observed and weighed regularly during the course of the experiment. Primary tumor growth was monitored at least once a week. Sixty days after tumor implantation, the mice were sacrificed using an overdose of pentobarbital. Final tumor volumes were determined by measuring the maximum and minimum tumor diameters using digital calipers; volume was calculated using the equation: tumor volume = $0.52a^2b$, where a and b represent the minimum and maximum tumor diameters, respectively (38). Matrigel implants were removed, fixed in 4% paraformaldehyde, processed for paraffin embedding, sectioned, and stained with Masson's trichrome.

In vivo angiogenesis was analyzed as previously described (39). Histological sections were scanned (40 \times objective and 10 \times ocular) for areas containing tumor associated blood vessels (researcher blinded to experimental condition). These areas were systematically imaged (160 \times magnification), and individual vessel counts for each field were documented to identify fields of maximum blood vessel density. Fields of maximum blood vessel density were statistically analyzed for between group differences; the data are expressed as the averages of three fields of maximum blood vessel density.

Active Cdc42 and Rac1 Assay—Measurement of active Cdc42 was performed essentially as previously described (12, 31). Briefly, the cells were washed and lysed in 500 μ l of buffer (20 mM Hepes, pH 7.4, 150 mM NaCl, 1% Nonidet P-40, 20 mM NaF, 20 μ M GTP, 1 mM MgCl₂, and protease inhibitors). After clarification by centrifugation and incubation with glutathione-

Sepharose, equal amounts of lysate were incubated with 40 μ g of GST-WASP-GBD. The complexes were collected with glutathione-Sepharose and resolved by SDS-PAGE and Western blotting. The blots were probed with anti-Cdc42 antibodies (BD Biosciences) and detected by ECL. In addition, 50 μ g of protein lysate was examined directly by blotting as whole cell lysate. Measurement of active Rac1 was performed by as outlined above for Cdc42, except GST-PAK-CRIB was used to isolate the GTP-bound protein, and the blots were probed with anti-Rac1 antibodies (BD Biosciences) (12, 40).

Invasion Assays—Matrigel invasion assays were performed using 24-well BD BioCoat Matrigel Invasion Chambers (Becton Dickinson Labware, Bedford, MA) according to the manufacturer's instructions. HEK-293H cells were transiently transfected with 2 μ g of a plasmid that expresses wild type IQGAP1, IQGAP1G75Q, IQGAP1MK24, or pcDNA3 (as a control). After 36 h, the cells were trypsinized and counted with a hemacytometer. For the invasion assay, 2×10^5 cells were resuspended in 500 μ l of medium containing 0.5% FBS and placed in the upper compartment of the chamber. The lower compartment was filled with 750 μ l of medium containing 10% FBS. After allowing cells to invade for 40 h, the cells on the upper surface of the Transwell were carefully removed with a cotton swab, and the membrane was fixed and stained with DiffQuick (Dade Behring). Counting was done in five randomly selected fields (magnification, 10 \times) within each well. In experiments with MEK inhibitor, 2×10^5 MCF/V or MCF/I cells were resuspended in 500 μ l of medium containing 1% FBS with 10 μ M U0126 (Promega) or 0.1% Me₂SO as a vehicle. The cells were placed in the upper compartment. The lower compartment was filled with 750 μ l of growth medium containing 10% FBS. After 2 days, the number of cells that invaded were stained and counted as described above.

Data Analysis—The data were analyzed using SigmaStat for Windows version 3.0.1a, and treatment groups (*i.e.* tumor cell lines: MCF/V, MCF/I, and MCF-silQ8) were compared using one-way analysis of variance. A probability of 0.05 was used in determining statistical significance.

RESULTS

Expression of IQGAP1 among Different Human Breast Cancer Cell Lines and Patient Tissue—IQGAP1 is overexpressed in several human neoplasms (16, 20, 22), but no published studies have examined breast carcinoma. Therefore, we determined the relative amounts of IQGAP1 among human breast epithelial cell lines. These cell lines can be divided into those that have estrogen receptors and progesterone receptors, namely MCF-7, T47D, ZR-75-1, and MDA-MB-361, and those lacking the receptors, namely MDA-MB-231, MDA-MB-435s, and Hs578T (41). Equal amounts of protein lysate from the cells were processed by Western blotting. Probing blots for tubulin verifies that equivalent amounts of protein are present in each sample (Fig. 1A). Analysis reveals that the amount of IQGAP1 in MCF-7, T47D, and ZR-75-1 cells is approximately equal (Fig. 1, A and B). Substantially less IQGAP1 is observed in MDA-MB-361, the other receptor-positive cell line. The reason for this finding is not known but may be because MDA-MB-361 is an adenocarcinoma (41). The highest IQGAP1 levels are

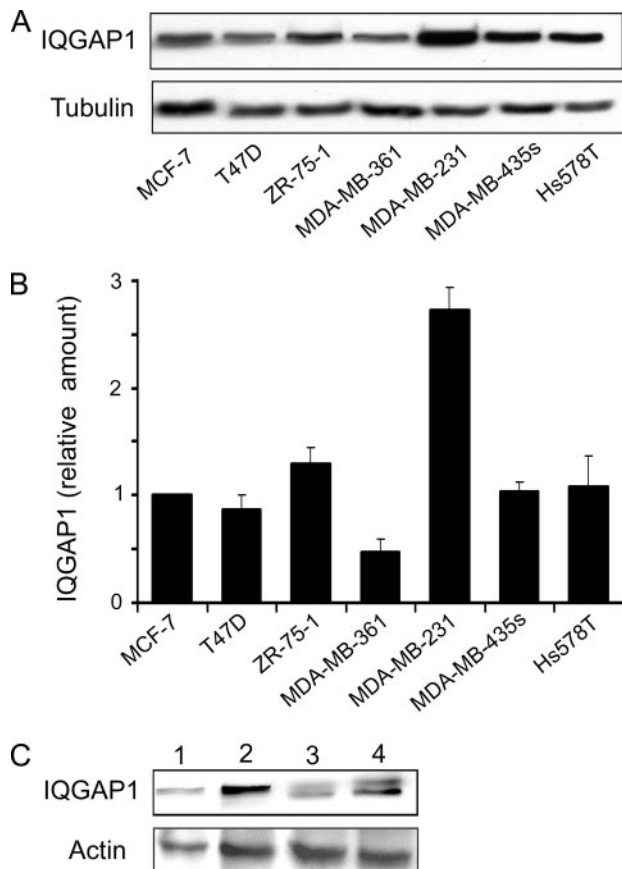


FIGURE 1. Expression of IQGAP1 in cultured human breast cells and breast tissue. A, the human breast epithelial cell lines indicated were grown in DMEM containing 10% serum. The cells were lysed, and equal amounts of protein lysate were resolved by SDS-PAGE and Western blotting. The blots were probed with anti-IQGAP1 and anti-tubulin antibodies, followed by horseradish peroxidase-conjugated secondary antibodies, and developed with ECL. B, the amount of IQGAP1 was quantified by densitometry and corrected for the amount of tubulin in the corresponding lysate. The data are expressed relative to the amount of IQGAP1 in MCF-7 cells and represent the means \pm S.E. ($n = 6$). C, equal amounts of breast protein lysate from two patients with infiltrating ductal carcinoma (lanes 2 and 4) and paired normal breast (lanes 1 and 3) were resolved by Western blotting. The blots were probed with anti-IQGAP1 antibody and visualized by ECL. After stripping, the blots were reprobed with anti-actin antibody.

detected in MDA-MB-231 cells, which have 2.7-fold more IQGAP1 than MCF-7 cells (Fig. 1, A and B). Importantly, these cells exhibit the highest invasive potential of 30 breast cell lines measured by modified Boyden chamber assays (42). The amounts of IQGAP1 in MDA-MB-435S and Hs578T cells are not different to those in MCF-7 cells. Several factors may account for this observation. Cluster analysis of MDA-MB-435S cells reveals that these cluster with melanoma cells and may not be of breast origin (43). Hs578T originates from a carcinosarcoma and is nontumorigenic in mice (41). Moreover, the expression levels of numerous genes differs among these cell lines (41, 42). Because a large number of factors contribute to invasion and metastasis (2, 44), it is not surprising that there is not a simple correlation of IQGAP1 levels with invasiveness.

These data reveal that breast epithelial cells have high levels of IQGAP1, with the highest concentrations found in the highly metastatic MDA-MB-231 cells. Our findings are supported by the recent comparison of three human breast epithelial cell lines, namely "near normal" MCF-10A, noninvasive BT474, and

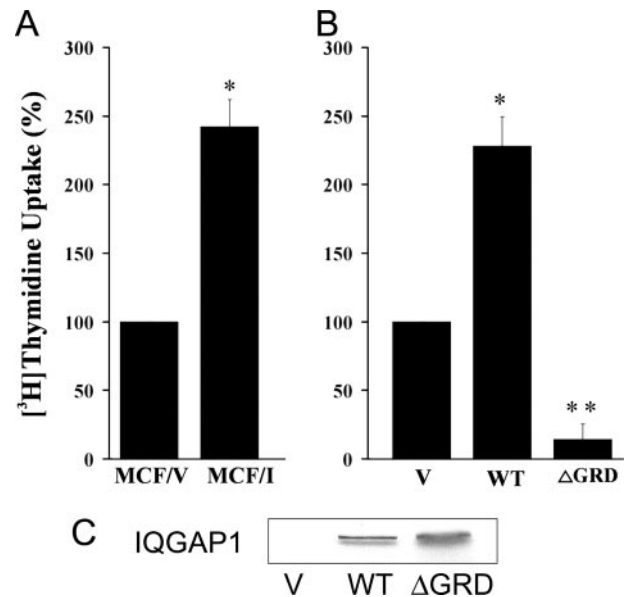


FIGURE 2. Effect of IQGAP1 on proliferation of MCF-7 cells. A, MCF-7 cells (2×10^5) stably expressing pcDNA3 vector (MCF/V) or Myc-tagged IQGAP1 (MCF/I) were seeded into 24-well culture dishes. After 24 h in DMEM containing 0.5% fetal calf serum, 1 μ Ci/ml [3 H]thymidine was added, and the cells were allowed to grow for 18 h. [3 H]thymidine incorporation was quantified as described under "Experimental Procedures." All of the assays were performed in quadruplicate. The data represent [3 H]thymidine uptake obtained relative to MCF/V cells. The means \pm S.E. are shown ($n = 12$ replications/group). *, $p < 0.005$. B, equal numbers of MCF-7 cells were transiently transfected with 10 μ g of vector (V), wild type (WT) IQGAP1, or IQGAP1 Δ GRD (Δ GRD). Cell proliferation was quantified as described for A. The data, expressed as [3 H]thymidine uptake relative to that in MCF/V cells, are the means \pm S.E. ($n = 3$, done in quadruplicate). *, $p < 0.0001$; **, $p < 0.005$. C, MCF-7 cells were transfected with pcDNA3 vector, wild type IQGAP1, or IQGAP1 Δ GRD. Equal amounts of protein lysate were resolved by SDS-PAGE, and Western blots were probed with anti-Myc antibody (all IQGAP1 constructs are Myc-tagged). A representative experiment is depicted.

metastatic MDA-MB-468 (45). Proteomic analysis shows that the amount of IQGAP1 in MDA-MB-468 cells is substantially higher than that in BT474 or MCF-10A cells.

To validate our findings with cultured cell lines, we examined the amount of IQGAP1 in human breast tissue. The levels of IQGAP1 in infiltrating ductal breast carcinoma from two patients were compared with levels in paired normal breast (Fig. 1C). Immunoblotting reveals that the amount of IQGAP1 in the carcinoma (Fig. 1C, lanes 2 and 4) is substantially greater than that in paired normal breast (Fig. 1C, lanes 1 and 3). The amounts of actin in the samples are similar. Collectively, these data suggest that IQGAP1 concentrations in breast carcinoma are higher than in normal breast and that highly metastatic breast epithelial cells contain more IQGAP1 than cells with low metastatic potential. Therefore, we manipulated the concentration of IQGAP1 in MCF-7 cells and examined the effects on tumorigenesis.

Effect of IQGAP1 on the Proliferative Response of Tumor Cells in Vitro—Incorporation of [3 H]thymidine was used to measure the proliferative capacity of MCF-7 cells stably expressing pcDNA3 vector (MCF/V), as controls, or Myc-tagged IQGAP1 (MCF/I). (MCF/I cells have 3-fold more IQGAP1 than MCF/V cells (12) (also see Figs. 6 and 7B).) The proliferative response was \sim 2.5-fold higher in MCF/I relative to MCF/V cells (Fig. 2A). The pattern of response was similar for transiently trans-

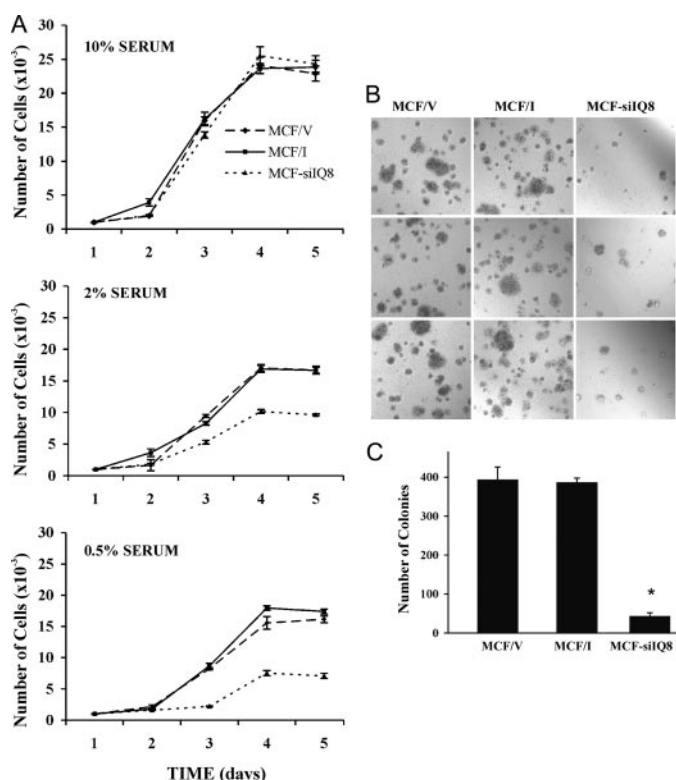


FIGURE 3. A role for IQGAP1 in *in vitro* tumorigenic growth of MCF-7 cells. A, 1×10^4 MCF/V, MCF/I or MCF-siQ8 cells were cultured in DMEM containing either 10, 2, or 0.5% serum. The cells were trypsinized and counted using a hemacytometer. The data represent the means \pm S.E., $n = 3$ replications (each done in triplicate) per group. The absence of error bars indicates that the S.E. is smaller than the size of the symbol. B, MCF/V, MCF/I, and MCF-siQ8 (1×10^4) cells were layered on soft agar as described under "Experimental Procedures." After incubating for 14 days at 37 °C in 5% CO₂, the formation of colonies was evaluated. Three representative images from each cell line are shown. The data are representative of four separate experiments. C, the total number of colonies >0.2 mm were counted using a light microscope, and differences between groups were compared. The data are expressed as the means \pm S.E., $n = 2$, performed in quadruplicate. *, $p < 0.0001$ relative to MCF/V-derived colonies.

fect cells. Thymidine incorporation into MCF-7 cells transiently overexpressing wild type IQGAP1 is significantly higher than those transiently transfected with vector (Fig. 2B). Similar analysis was performed using IQGAP1ΔGRD, an IQGAP1 mutant that functions as a dominant negative construct (11). Transient transfection of IQGAP1ΔGRD markedly (86 \pm 11.3%) reduces proliferation of MCF-7 cells (Fig. 2B). Western blotting reveals that wild type IQGAP1 and IQGAP1ΔGRD are expressed at equivalent levels in the transiently transfected cells (Fig. 2C). Together, these data suggest a positive association between IQGAP1 expression and *in vitro* proliferation of MCF-7 cells.

Effect of IQGAP1 on *in Vitro* Proliferative Growth and Transformation—Serum-dependent proliferative growth was evaluated as a measure of cellular transformation. In addition to MCF/V and MCF/I cells, we used MCF-7 cells with stable integration into the genome of siRNA for IQGAP1. Termed MCF-siQ8, these cells have 80% reduction in IQGAP1 expression (12) (also see Fig. 6). Equal numbers of cells were plated and cultured in 10, 2, or 0.5% serum. At 2-day intervals, the cells were trypsinized and counted. When cultured under optimal conditions (*i.e.* 10% serum), MCF/V, MCF/I, and MCF-siQ8 cell lines have similar growth rates (Fig. 3A). At lower concen-

trations of serum, the rate of growth of MCF/V cells is essentially the same as that of MCF/I cells. In contrast, growth of MCF-siQ8 cells is reduced substantially under suboptimal culture conditions (*i.e.* at 2% and 0.5% serum) (Fig. 3A). To validate these findings, analysis was repeated by an alternative method, namely the MTT assay. In this assay, the cells were grown in 96-well plates, and proliferation was quantified after 24 h of growth under optimal and suboptimal conditions. The MTT proliferation assay yielded a pattern of response similar to that seen with thymidine uptake (data not shown).

To further examine the involvement of IQGAP1 in cellular transformation, the three MCF-7 cell lines were assayed for anchorage-independent growth when suspended in soft agar. This assay provides a stringent *in vitro* measure of the transformed phenotypes typically observed in malignant cells (37). Given that all three cell lines were derived from the MCF-7 human breast carcinoma cell line, it is not surprising that MCF/V, MCF/I, and MCF-siQ8 cells all exhibit anchorage-independent cell growth (Fig. 3B). Nevertheless, knockdown of IQGAP1 markedly reduces the ability of MCF-7 cells to form colonies in soft agar (Fig. 3, B and C). Together, the similar patterns of response from serum-dependent and anchorage-independent growth assays strongly suggest that IQGAP1 contributes to the transformed phenotype of MCF-7 cells.

IQGAP1 Promotes *in Vivo* Tumorigenesis—Given the evidence suggesting a positive association between IQGAP1 expression and the *in vitro* proliferative growth and transformation of MCF-7 cells, we then addressed the role of IQGAP1 in *in vivo* tumorigenesis. MCF/V, MCF/I, and MCF-siQ8 cells were suspended in Matrigel, and 1×10^5 cells were injected subcutaneously into immunocompromised female mice. For each group, the rate of appearance of primary tumors was monitored, and final tumor volumes were obtained to determine whether IQGAP1 expression alters *in vivo* growth characteristics of primary, subcutaneous tumors.

Weekly inspection of subcutaneous implants suggested a positive association between IQGAP1 expression and the proliferative growth of *in vivo* tumors (Fig. 4); this relationship was apparent as early as 1 week post-implantation and continued throughout the course of the experiment. When compared with implants derived from MCF/V cells, those derived from MCF/I cells grew faster, resulting in more visible, palpable tumors/group (Fig. 4A). By 5 weeks palpable tumors were detected in all mice injected with MCF/I cells, but only 70% of those injected with MCF/V cells. The latency period of MCF-siQ8-derived tumors was longer, and fewer palpable tumors were always visible in this group (Fig. 4A). Only 20% of the mice injected with MCF-siQ8 cells developed palpable tumors. The data pertaining to the final volumes of the tumors are consistent with soft agar results. The final volume of MCF/I-derived tumors did not differ from those of MCF/V tumors (Fig. 4B). However, MCF-siQ8-derived tumors were significantly smaller than those derived from MCF/V and MCF/I cells (Fig. 4B). Therefore, it appears that IQGAP1 contributes to the tumorigenic growth of MCF-7 cells *in vivo*.

Tumor Invasion and Angiogenesis—Histologic examination at 60 days of tumors derived from MCF/V cells reveal that the cells proliferate throughout the Matrigel and grow in host tis-

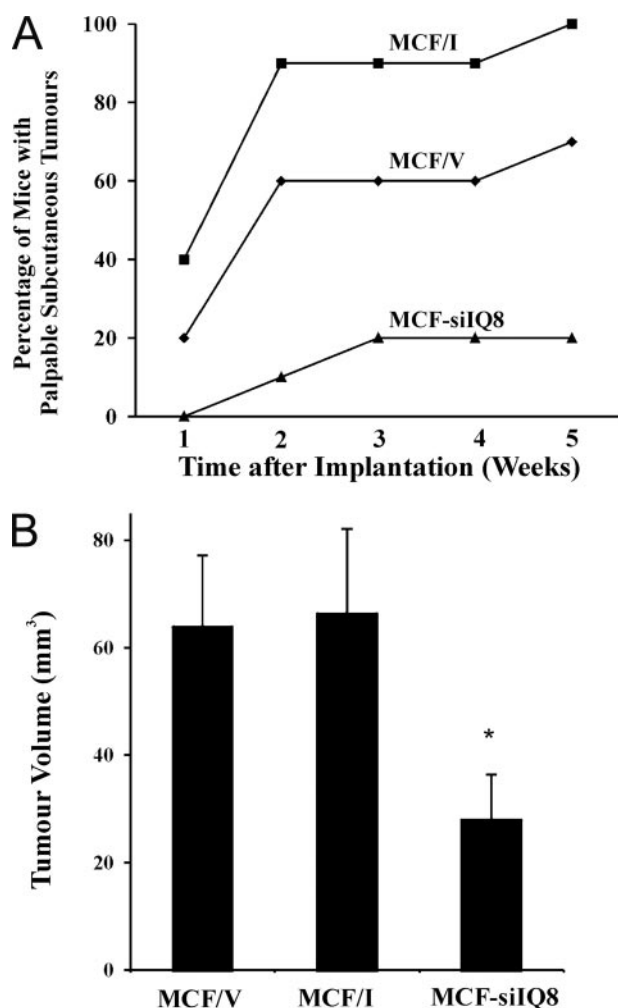


FIGURE 4. IQGAP1 promotes *in vivo* tumorigenic growth of MCF-7 cells. A, immunocompromised NOD.CB17-Prkdc^{scid}/JCH3H/HeJ mice received subcutaneous injections of equal numbers (1×10^5) of MCF/V, MCF/I, or MCF-silQ8 cells suspended in Matrigel; rate of appearance of palpable primary tumors was examined. B, final volume of tumors derived from subcutaneous implants. Primary tumor volumes were measured 60 days after transplantation of MCF/V, MCF/I, or MCF-silQ8 cells. The data represent the means \pm S.E., $n = 10$ animals/group. Tumor volumes were significantly lower in mice receiving MCF-silQ8 transplants relative to those receiving MCF/I ($p < 0.05$) or MCF/V ($p < 0.05$) transplants. Final tumor volumes in mice receiving MCF/I and MCF/V transplants did not differ ($p = 0.908$).

sue but do not invade skeletal muscle (Fig. 5A). In contrast, MCF/I tumors are highly invasive and infiltrate extensively through the mouse skeletal muscle. Tumors from MCF-silQ8 cells remained small and did not extend beyond the Matrigel plug (Fig. 5A).

Angiogenesis was determined by quantifying neovascularization in tumors as described (39). This assay is based on the angiogenesis that occurs in growth factor-reduced Matrigel. The angiogenic response is evaluated by examining the gross morphology of the Matrigel implants and quantifying new vessel formation in sections stained with Masson's trichrome. The neovascular response in primary tumors derived from MCF/I cells is significantly higher than that derived from MCF/V cells (Fig. 5B). Angiogenesis in MCF-silQ8 tumors is less than that in MCF/V tumors, but the difference is not statistically significant.

A number of binding partners of IQGAP1 are potential candidate molecules for involvement in the mechanism by which IQGAP1 promotes tumorigenesis. We examined the participation of some of these in cell proliferation and invasion.

Altering IQGAP1 Concentration in MCF-7 Cells Alters the Amounts of Active Cdc42 and Rac1—IQGAP1 binds directly to Cdc42 and Rac1 *in vitro*, stabilizing the GTPases in their active form (11, 25). Stable overexpression of IQGAP1 in MCF-7 cells increases the amounts of active Cdc42 and Rac1 (Fig. 6) (12). Consistent with these findings, stable knockdown of IQGAP1 substantially reduces the amounts of GTP-bound Cdc42 and Rac1 in MCF-7 cells (Fig. 6). These data suggest that Cdc42 and Rac1 contribute to the mechanism by which IQGAP1 enhances tumorigenesis of breast epithelial cells. This possibility was explored further using complementary strategies.

Cdc42 and Rac1 Participate in IQGAP1-mediated Increase in Cell Proliferation—The possible participation of Cdc42 and Rac1 in IQGAP1-stimulated proliferation was examined with dominant negative constructs. N17Cdc42 and N17Rac1 markedly impair proliferation of cells overexpressing IQGAP1 (Fig. 7A, right panel). This effect is particularly evident at 72 h. Proliferation at 72 h of MCF/I cells transfected with N17Cdc42 or N17Rac1 is approximately the same as proliferation of vector-transfected MCF/I cells at 24 h (Fig. 7A, right panel). Although the dominant negative constructs also attenuate proliferation of MCF/V cells, the magnitude of the reduction is substantially less than that seen with MCF/I cells (Fig. 7A, left panel). (IQGAP1 does not bind RhoA (7), so we did not examine this GTPase.) Western blotting verifies the 3-fold overexpression of IQGAP1 in MCF/I cells (compared with MCF/V cells) and that the dominant negative Cdc42 and Rac1 constructs are expressed (Fig. 7B). Probing blots for tubulin reveals that protein loading was equivalent among samples. These data, combined with the results presented in Figs. 2 and 6, suggest that IQGAP1 increases cell proliferation, at least in part, in a Cdc42- and Rac1-dependent manner.

Binding to Actin and Cdc42/Rac1 Is Required for IQGAP1 to Promote Cell Invasion—The mechanism by which IQGAP1 promotes cell invasion was also investigated. Using dominant negative constructs, we previously documented that IQGAP1 augments invasion of MCF-7 cells, at least in part, via Cdc42 and Rac1 (12). We used mutant IQGAP1 constructs to gain further insight into which binding partners are necessary for IQGAP1 to enhance cell invasion. IQGAP1G75Q, a point mutant that lacks binding to actin (28), and IQGAP1ΔMK24, which is unable to bind Cdc42 or Rac1 (29), were used. Transient overexpression of wild type IQGAP1 increases cell invasion, by ~ 2.5 -fold (Fig. 8A). In contrast, neither IQGAP1G75Q nor IQGAP1ΔMK24 is able to significantly enhance cell invasion (Fig. 8). Western blotting reveals that the expression level of the IQGAP1 constructs is equivalent (Fig. 8B). These data strongly suggest that binding to actin and Cdc42 and/or Rac1 is necessary for IQGAP1 to maximally promote cell invasion.

Inhibition of MAPK Reduces IQGAP1-stimulated Cell Invasion—More recently, we observed that IQGAP1 is a scaffold in the MAPK signaling pathway (13–15). The ERK inhibitor U0126 was used to evaluate the possible participation of the MAPK pathway in the mechanism by which IQGAP1 increases

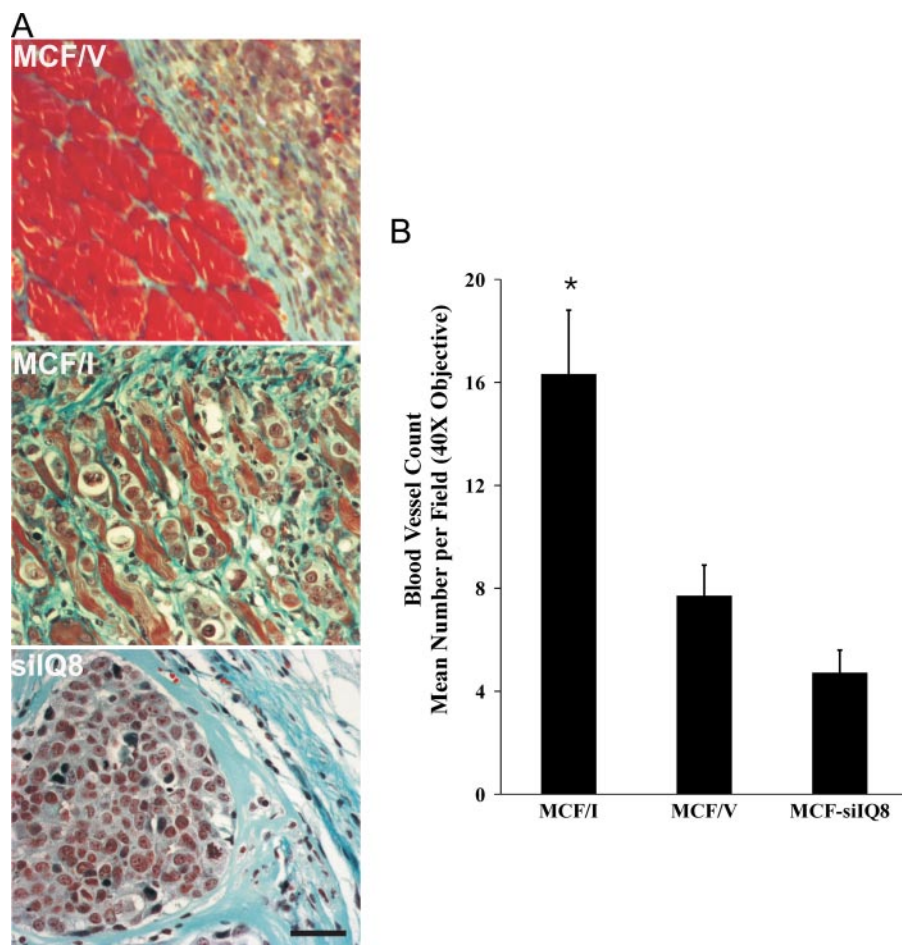


FIGURE 5. IQGAP1 promotes invasion of MCF-7 cells in mice. A, Masson's trichrome staining of representative tumors at 60 days from immunocompromised mice injected with MCF/V, MCF/I, or MCF-silQ8 (silQ8) cells. MCF/V cells proliferate but do not invade host skeletal muscle. MCF/I cells show extensive invasion of host tissue with growth visible in skeletal muscle. MCF-silQ8 cells remain confined to the Matrigel plug. Scale bar, 100 μ m. B, quantification of tumor-induced neovascularization in sections stained with Masson's trichrome. Neovascularization in tumors derived from MCF/I, MCF/V, and MCF-silQ8 cells was determined as described under "Experimental Procedures." The data are expressed as the mean number of microvessels in three fields of maximum blood vessel density (mean \pm S.E., $n = 10$ animals/group, 160 \times magnification). The neovascular response was higher in primary tumors derived from MCF/I cells relative to those derived from MCF/V ($p < 0.05$) and MCF-silQ8 ($p < 0.05$) cells. The amount of neovascularization in MCF/V- and MCF-silQ8-derived implants did not differ significantly ($p = 0.341$).

cell invasion. Stable overexpression of IQGAP1 promotes an ~ 3 -fold increase in invasion of MCF-7 cells into Matrigel (Fig. 9). Incubation of MCF/I cells with 10 μ M U0126 completely eliminates IQGAP1-stimulated invasion (Fig. 9). Although U0126 also reduces invasion of MCF/V cells, the extent of the reduction is substantially less than that produced in MCF/I cells (Fig. 9). These data suggest that the MAPK pathway contributes to the invasion of MCF-7 cells produced by IQGAP1.

DISCUSSION

An accumulating body of evidence has documented that IQGAP1 levels are increased in solid neoplasms derived from a number of types of tissue. IQGAP1 overexpression, both RNA and protein, has been reported in several malignant tumors (5). In addition, analysis by immunohistochemistry of tissues obtained from patients reveals that localization of IQGAP1 provides prognostic information for at least some carcinomas (20, 22). Despite these findings, the data are circumstantial, and

no prior studies have directly evaluated whether IQGAP1 promotes tumorigenesis. By differentially regulating the amount of IQGAP1 in human breast epithelial cells, we document here that IQGAP1 directly contributes to tumorigenesis. Overexpression of IQGAP1 enhances cell proliferation, whereas IQGAP1 knockdown reduces *in vitro* assays of tumorigenesis. Consistent with these findings, manipulation of intracellular IQGAP1 concentrations alters tumorigenicity of MCF-7 cells in mice.

Knockdown of endogenous IQGAP1 attenuates tumorigenicity of MCF-7 cells. Cells with reduced IQGAP1 concentrations have an impaired ability to grow at low concentrations of serum. Similarly, growth of MCF-7 cells in soft agar and in immunocompromised mice, both formation of tumors and invasion of host tissue, are markedly impaired when IQGAP1 concentrations are lowered. As anticipated, overexpression of IQGAP1 does not augment the *in vitro* growth characteristics of the malignant MCF-7 cells. Nevertheless, MCF/I cells exhibit increased invasion of host tissue when injected into immunocompromised mice. The increased invasion strongly suggests that the tumors are more aggressive. Invasion and metastasis, complex and closely allied processes, are the cause of 90% of human cancer deaths (46). IQGAP1 is important

for cell migration (12, 47, 48), suggesting a possible mechanism for tumor invasion. Congruent with this hypothesis, we previously observed that overexpression of IQGAP1 promotes invasion of MCF-7 cells *in vitro*, whereas the dominant negative IQGAP1 Δ GRD reduced invasion of T47D cells (12). In this study we observe that overexpression of IQGAP1 also significantly increases angiogenesis in the mouse model. Primary tumors derived from MCF/I cells exhibit an ~ 2 -fold increase in blood vessel formation over MCF/V cells. The mechanism underlying this observation is not known. It is tempting to speculate that the previously described interaction of IQGAP1 with the vascular endothelial growth factor receptor (49) promotes tumor angiogenesis. However, caution should be exercised in drawing this conclusion. It is conceivable that the increased neovascularization we observed with tumors derived from MCF/I cells may simply be the consequence of increased invasion.

Many binding partners of IQGAP1 are implicated in the development of cancer (7), and it seems reasonable to postulate

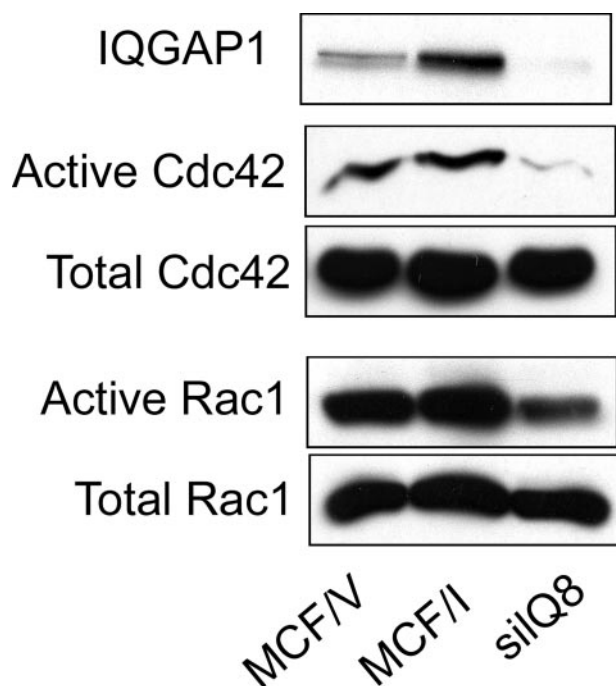


FIGURE 6. Altering IQGAP1 concentrations in MCF-7 cells alters the amounts of active Cdc42 and Rac1. Equal numbers of MCF/V, MCF/I, and MCF-silQ8 cells were cultured in DMEM. The cells were lysed, equal amounts of protein lysate were resolved by SDS-PAGE, and the blots were probed with anti-Cdc42 (Total Cdc42), anti-Rac1 (Total Rac1), or anti-IQGAP1 antibodies. Equal amounts of protein were also incubated with GST-WASP-GBD or GST-PAK-CRIB to measure active Cdc42 and Rac1, respectively. The complexes were collected with glutathione-Sepharose and resolved by SDS-PAGE, and the blots were probed with anti-Cdc42 or anti-Rac1 antibodies. The data are representative of two independent experimental determinations.

that several of these may contribute to the mechanism by which IQGAP1 enhances tumorigenesis. These molecules include calmodulin, Rac1, Cdc42, E-cadherin, β -catenin, components of the MAPK pathway, and adenomatous polyposis coli. Examination of all these is a large undertaking, which is beyond the scope of the present work. The documented involvement of IQGAP1 in both MAPK signaling (13–15, 50) and in the function of the Rho GTPases Cdc42 and Rac1 (11, 12, 25, 33) led us to examine the potential role of those proteins in IQGAP1-stimulated tumorigenesis. Ras signaling pathways are aberrant in many human tumors, with oncogene activation reported in ~30% of these (51). Although mutations of Ras are not associated with the majority of breast cancer, over 50% of human breast cancer has increased activation of Ras (52, 53). Several effectors are involved in Ras-induced transformation, including the MAPK pathway, phosphatidylinositol 3-kinase, and Rho GTPases (54, 55). The MEK/ERK pathway regulates cell proliferation (56) and oncogenic transformation (57). We selected the widely used inhibitor U0126, which inhibits MEK activation and MEK catalytic activity, to gain insight into the involvement of the MAPK pathway. Inhibition of MAPK signaling abrogated the increased invasion mediated by IQGAP1. Although U0126 also attenuated invasion of MCF-7 cells, the magnitude of the reduction was substantially less than that seen with MCF/I cells. These data imply that the MAPK cascade contributes to the mechanism by which IQGAP1 promotes invasion of breast carcinoma cells.

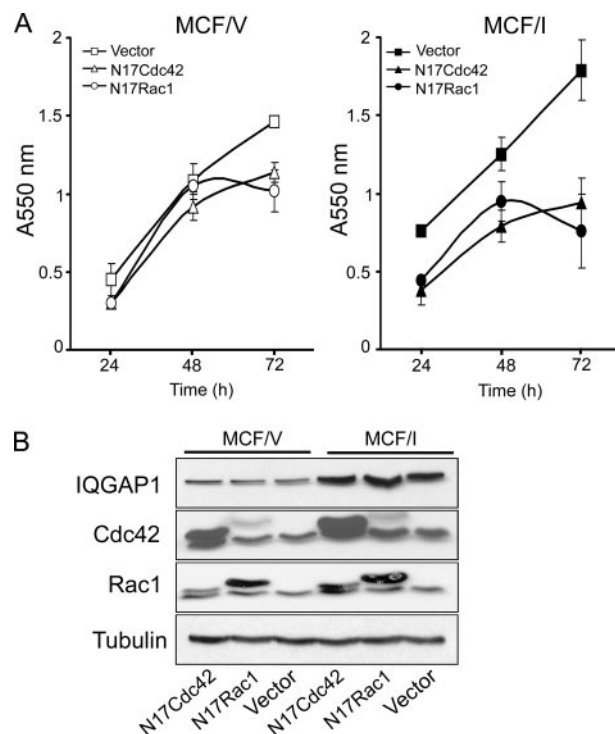


FIGURE 7. Cdc42 and Rac1 participate in IQGAP1-mediated increase in cell proliferation. MCF/V and MCF/I cells were transiently transfected with 1 μ g of empty pcDNA3 vector, N17Cdc42, or N17Rac1. **A**, after 36 h, 5×10^3 cells were plated in tissue culture plates for 24, 48, or 72 h. Proliferation was determined using the MTT assay as described under “Experimental Procedures.” The data are the means \pm S.D. of assays performed in triplicate and are representative of two independent experimental determinations. The absence of error bars indicates that the S.D. is smaller than the size of the symbol. **B**, equal numbers of transfected MCF/V and MCF/I cells were lysed and processed by SDS-PAGE and Western blotting. The blots were probed with antibodies to IQGAP1, Cdc42, Rac1, and tubulin. The data are representative of two independent experiments.

There is increasing evidence that Rho proteins are involved in almost every stage of tumorigenesis (58). The Rho proteins are members of the Ras superfamily of GTPases, which act as molecular switches to control a wide range of essential biochemical pathways (59). The GTPases are inactive when bound to GDP. Guanine nucleotide exchange factors catalyze the release of GDP, allowing GTP (which is in excess) to bind. The active, GTP-bound form binds target proteins, eliciting cellular responses. Inactivation is augmented by GTPase-activating proteins, which increase the hydrolysis of GTP to GDP by an intrinsic GTPase. The Rho subfamily contains several members, the best characterized of which are RhoA, Rac1, and Cdc42 (60). In addition to regulating the actin cytoskeleton and cell morphology, Rho GTPases affect gene expression, cell proliferation, and cell survival, cellular functions important in tumorigenesis (58). Consistent with these actions, a large body of evidence supports the involvement of Rho proteins in several types of cancer (58). Activated Rho mutant constructs can transform fibroblasts, whereas dominant negative mutants block transformation by Ras (58). Moreover, Rho proteins promote the metastasis of tumor cells, including breast cancer (58, 61). Importantly, deregulation of both Rac1 and Cdc42 has been reported in breast carcinoma (58, 62). Coordinated activation and functional co-operation occurs between the Ras and

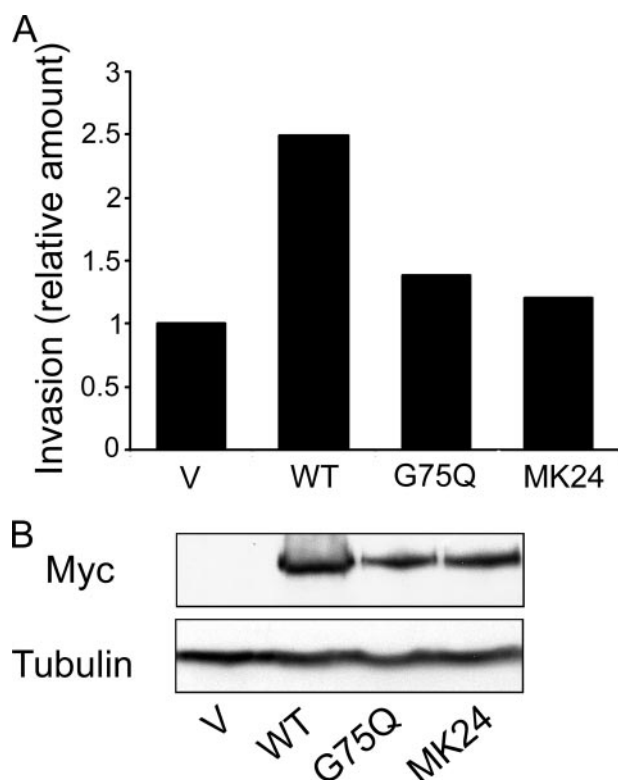


FIGURE 8. Binding to Cdc42/Rac1 and actin is required for IQGAP1 to maximally augment cell invasion. HEK-293H cells were transiently transfected with equal amounts of empty pcDNA3 vector (V), wild type IQGAP1 (WT), IQGAP1G75Q (G75Q), or IQGAP1ΔMK24 (MK24). After 36 h, the cells were trypsinized and counted. *A*, 2×10^5 cells were suspended in 500 μ l of DMEM/0.5% FBS and placed in the upper chamber of a 24-well Matrigel invasion chamber. The number of cells that invaded into the Matrigel in 48 h was quantified as described under "Experimental Procedures." All of the assays were performed in duplicate or triplicate. The data are expressed relative to invasion by cells transfected with vector and are representative of four independent experimental determinations. *B*, equal numbers of cells were lysed and processed by Western blotting. The blots were probed with anti-Myc antibody (all IQGAP1 constructs are Myc-tagged) and tubulin (as loading control). A representative experiment is shown.

Rho GTPases (59). The transforming activity of Ras requires Rac1 and Cdc42 (59, 63). We show here that knockdown of IQGAP1, which reduces MCF-7 cell proliferation *in vitro* and tumorigenesis *in vivo*, substantially reduces the amount of active Cdc42 and Rac1 in breast carcinoma cells. Consistent with these findings, dominant negative Cdc42 and Rac1 impair IQGAP1-stimulated proliferation of MCF-7 cells. Moreover, Cdc42/Rac1 are necessary for IQGAP1 to promote cell invasion. A mutant IQGAP1 construct that selectively lacks binding to Cdc42 and Rac1 (29), termed IQGAP1ΔMK24, is unable to increase cell invasion. Collectively these data suggest that Cdc42 and Rac1 participate in both IQGAP1-stimulated tumorigenesis and invasion.

Recent evidence reveals that binding to actin is required for IQGAP1 to promote cell motility. IQGAP1G75Q, a point mutant construct that cannot bind actin, does not increase cell motility (28). Concordant with these observations, we observe here that IQGAP1G75Q fails to increase cell invasion. Thus, an interaction with actin is also necessary for IQGAP1 to enhance invasion. It is important to bear in mind that our observations do not preclude a role for (an)other protein(s) in the mechanism by which IQGAP1 promotes tumorigenesis of breast epi-

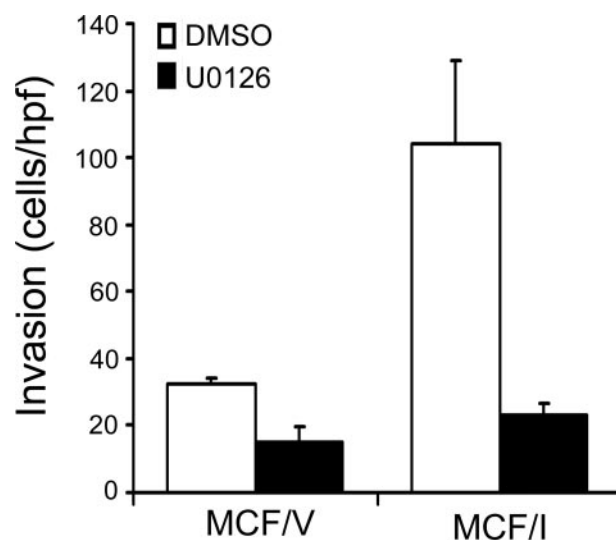


FIGURE 9. The MAPK inhibitor U0126 reduces IQGAP1-stimulated invasion of MCF-7 cells. MCF/V and MCF/I cells (2×10^5 each) were suspended in 500 μ l of DMEM/1% FBS with vehicle (Me₂SO) or 10 μ M U0126 and placed in the upper compartment of 24-well Matrigel Invasion Chambers. The number of cells that invaded into the Matrigel in 48 h was quantified as described under "Experimental Procedures." All of the assays were performed in duplicate or triplicate. The data are expressed as the number of invading cells/high power field (hpf) and are the means \pm S.D. of two independent experimental determinations, with at least five separate fields counted in each assay.

thelium. It is possible, perhaps even likely, that other IQGAP1-binding partners, such as β -catenin or E-cadherin, both of which are implicated in neoplastic transformation (64, 65), contribute to IQGAP1-induced tumorigenesis. Additional studies are necessary to test this hypothesis.

Regardless of the mechanism, our data document for the first time that IQGAP1 stimulates cell proliferation and promotes tumorigenesis in an *in vivo* model. An elegant study from Richard Hynes's group identified that IQGAP1 mRNA is up-regulated in metastasis (19). Microarray analysis of genes selectively up-regulated in metastatic melanoma revealed that only 32 were up-regulated >2.5 -fold; one of these was IQGAP1. These *in vivo* observations are supported by *in vitro* analyses revealing that overexpression of IQGAP1 enhances motility and invasion of breast epithelial cells, whereas knockdown of endogenous IQGAP1 reduces motility and invasion (12). Collectively the findings presented in this manuscript, in conjunction with previously published data, support the concept that IQGAP1 participates in both transformation and metastasis, suggesting that it may be an appealing therapeutic target for carcinoma.

Acknowledgments—We thank Chris French for helpful discussions. We appreciate the expert help of Rob Krikorian in the preparation of the manuscript.

REFERENCES

1. Fidler, I. J. (2002) *Semin. Cancer Biol.* **12**, 89–96
2. Fidler, I. J. (2003) *Nat. Rev. Cancer* **3**, 453–458
3. Gupta, G. P., and Massague, J. (2006) *Cell* **127**, 679–695
4. Briggs, M. W., and Sacks, D. B. (2003) *FEBS Lett.* **542**, 7–11
5. Briggs, M. W., and Sacks, D. B. (2003) *EMBO Rep.* **4**, 571–574
6. Mateer, S. C., Wang, N., and Bloom, G. S. (2003) *Cell Motil. Cytoskeleton* **55**, 147–155
7. Brown, M. D., and Sacks, D. B. (2006) *Trends Cell Biol.* **16**, 242–249

8. Jeong, H. W., Li, Z., Brown, M. D., and Sacks, D. B. (2007) *J. Biol. Chem.* **282**, 20752–20762
9. Kuroda, S., Fukata, M., Nakagawa, M., Fujii, K., Nakamura, T., Ookubo, T., Izawa, I., Nagase, T., Nomura, N., Tani, H., Shoji, I., Matsuura, Y., Yonehara, S., and Kaibuchi, K. (1998) *Science* **281**, 832–835
10. Briggs, M. W., Li, Z., and Sacks, D. B. (2002) *J. Biol. Chem.* **277**, 7453–7465
11. Swart-Mataraza, J. M., Li, Z., and Sacks, D. B. (2002) *J. Biol. Chem.* **277**, 24753–24763
12. Mataraza, J. M., Briggs, M. W., Li, Z., Entwistle, A., Ridley, A. J., and Sacks, D. B. (2003) *J. Biol. Chem.* **278**, 41237–41245
13. Roy, M., Li, Z., and Sacks, D. B. (2004) *J. Biol. Chem.* **279**, 17329–17337
14. Roy, M., Li, Z., and Sacks, D. B. (2005) *Mol. Cell. Biol.* **25**, 9740–9752
15. Ren, J. G., Li, Z., and Sacks, D. B. (2007) *Proc. Natl. Acad. Sci. U. S. A.* **104**, 10465–10469
16. Sugimoto, N., Imoto, I., Fukuda, Y., Kurihara, N., Kuroda, S., Tanigami, A., Kaibuchi, K., Kamiyama, R., and Inazawa, J. (2001) *J. Hum. Genet.* **46**, 21–25
17. Sun, W., Zhang, K., Zhang, X., Lei, W., Xiao, T., Ma, J., Guo, S., Shao, S., Zhang, H., Liu, Y., Yuan, J., Hu, Z., Ma, Y., Feng, X., Hu, S., Zhou, J., Cheng, S., and Gao, Y. (2004) *Cancer Lett.* **212**, 83–93
18. Bertucci, F., Salas, S., Eysteries, S., Nasser, V., Finetti, P., Ginestier, C., Charafe-Jauffret, E., Lloriod, B., Bachelart, L., Montfort, J., Victorero, G., Viret, F., Ollendorff, V., Fert, V., Giovaninni, M., Delpero, J. R., Nguyen, C., Viens, P., Monges, G., Birnbaum, D., and Houlgatte, R. (2004) *Oncogene* **23**, 1377–1391
19. Clark, E. A., Golub, T. R., Lander, E. S., and Hynes, R. O. (2000) *Nature* **406**, 532–535
20. Nabeshima, K., Shimao, Y., Inoue, T., and Kono, M. (2002) *Cancer Lett.* **176**, 101–109
21. Miyoshi, T., Shirakusa, T., Ishikawa, Y., Iwasaki, A., Shiraishi, T., Maki-moto, Y., Iwasaki, H., and Nabeshima, K. (2005) *Pathol. Int.* **55**, 419–424
22. Dong, P., Nabeshima, K., Nishimura, N., Kawakami, T., Hachisuga, T., Kawarabayashi, T., and Iwasaki, H. (2006) *Cancer Lett.* **243**, 120–127
23. Balenci, L., Clarke, I. D., Dirks, P. B., Assard, N., Ducray, F., Jouvett, A., Belin, M. F., Honnorat, J., and Baudier, J. (2006) *Cancer Res.* **66**, 9074–9082
24. Takemoto, H., Doki, Y., Shiozaki, H., Imamura, H., Utsunomiya, T., Miyata, H., Yano, M., Inoue, M., Fujiwara, Y., and Monden, M. (2001) *Int. J. Cancer* **91**, 783–788
25. Hart, M. J., Callow, M. G., Souza, B., and Polakis, P. (1996) *EMBO J.* **15**, 2997–3005
26. Ho, Y. D., Joyal, J. L., Li, Z., and Sacks, D. B. (1999) *J. Biol. Chem.* **274**, 464–470
27. Sokol, S. Y., Li, Z., and Sacks, D. B. (2001) *J. Biol. Chem.* **276**, 48425–48430
28. Mataraza, J. M., Li, Z., Jeong, H. W., Brown, M. D., and Sacks, D. B. (2007) *Cell Signal.* **19**, 1857–1865
29. Mataraza, J. M., Briggs, M. W., Li, Z., Frank, R., and Sacks, D. B. (2003) *Biochem. Biophys. Res. Commun.* **305**, 315–321
30. Nobes, C. D., and Hall, A. (1995) *Cell* **81**, 53–62
31. Kim, S. H., Li, Z., and Sacks, D. B. (2000) *J. Biol. Chem.* **275**, 36999–37005
32. Li, Z., Kim, S. H., Higgins, J. M., Brenner, M. B., and Sacks, D. B. (1999) *J. Biol. Chem.* **274**, 37885–37892
33. Joyal, J. L., Annan, R. S., Ho, Y. D., Huddleston, M. E., Carr, S. A., Hart, M. J., and Sacks, D. B. (1997) *J. Biol. Chem.* **272**, 15419–15425
34. Joyal, J. L., and Sacks, D. B. (1994) *J. Biol. Chem.* **269**, 30039–30048
35. Sacks, D. B., and McDonald, J. M. (1992) *Arch. Biochem. Biophys.* **299**, 275–280
36. Vadlamudi, R. K., Adam, L., Wang, R. A., Mandal, M., Nguyen, D., Sahin, A., Chernoff, J., Hung, M. C., and Kumar, R. (2000) *J. Biol. Chem.* **275**, 36238–36244
37. Cox, A. D., and Der, C. J. (1994) *Methods Enzymol.* **238**, 277–294
38. Baguley, B. C., Calveley, S. B., Crowe, K. K., Fray, L. M., O'Rourke, S. A., and Smith, G. P. (1989) *Eur. J. Cancer Clin. Oncol.* **25**, 263–269
39. Jadeski, L. C., and Lala, P. K. (1999) *Am. J. Pathol.* **155**, 1381–1390
40. Brown, M. D., Bry, L., Li, Z., and Sacks, D. B. (2007) *J. Biol. Chem.* **282**, 30265–30272
41. Lacroix, M., and Leclercq, G. (2004) *Breast Cancer Res. Treat.* **83**, 249–289
42. Neve, R. M., Chin, K., Fridlyand, J., Yeh, J., Baehner, F. L., Fevr, T., Clark, L., Bayani, N., Coppe, J. P., Tong, F., Speed, T., Spellman, P. T., DeVries, S., Lapuk, A., Wang, N. J., Kuo, W. L., Stilwell, J. L., Pinkel, D., Albertson, D. G., Waldman, F. M., McCormick, F., Dickson, R. B., Johnson, M. D., Lippman, M., Ethier, S., Gazdar, A., and Gray, J. W. (2006) *Cancer Cell* **10**, 515–527
43. Ross, D. T., Scherf, U., Eisen, M. B., Perou, C. M., Rees, C., Spellman, P., Iyer, V., Jeffrey, S. S., Van de Rijn, M., Waltham, M., Pergamenschikov, A., Lee, J. C., Lashkari, D., Shalon, D., Myers, T. G., Weinstein, J. N., Botstein, D., and Brown, P. O. (2000) *Nat. Genet.* **24**, 227–235
44. Pantel, K., and Brakenhoff, R. H. (2004) *Nat. Rev. Cancer* **4**, 448–456
45. Kulasingam, V., and Diamandis, E. P. (2007) *Mol. Cell. Proteomics* **6**, 1997–2011
46. Hanahan, D., and Weinberg, R. A. (2000) *Cell* **100**, 57–70
47. Watanabe, T., Wang, S., Noritake, J., Sato, K., Fukata, M., Takefuji, M., Nakagawa, M., Izumi, N., Akiyama, T., and Kaibuchi, K. (2004) *Dev. Cell* **7**, 871–883
48. Kholmanskikh, S. S., Koeller, H. B., Wynshaw-Boris, A., Gomez, T., Le-tourneau, P. C., and Ross, M. E. (2006) *Nat. Neurosci.* **9**, 50–57
49. Yamaoka-Tojo, M., Ushio-Fukai, M., Hilenski, L., Dikalov, S. I., Chen, Y. E., Tojo, T., Fukai, T., Fujimoto, M., Patrushev, N. A., Wang, N., Kontos, C. D., Bloom, G. S., and Alexander, R. W. (2004) *Circ. Res.* **95**, 276–283
50. Bourguignon, L. Y., Gilad, E., Rothman, K., and Peyrollier, K. (2005) *J. Biol. Chem.* **280**, 11961–11972
51. Downward, J. (2003) *Nat. Rev. Cancer* **3**, 11–22
52. Eckert, L. B., Repasky, G. A., Ulku, A. S., McFall, A., Zhou, H., Sartor, C. I., and Der, C. J. (2004) *Cancer Res.* **64**, 4585–4592
53. von Lintig, F. C., Dreilinger, A. D., Varki, N. M., Wallace, A. M., Casteel, D. E., and Boss, G. R. (2000) *Breast Cancer Res. Treat.* **62**, 51–62
54. Campbell, S. L., Khosravi-Far, R., Rossman, K. L., Clark, G. J., and Der, C. J. (1998) *Oncogene* **17**, 1395–1413
55. Marshall, C. J. (1996) *Curr. Opin. Cell Biol.* **8**, 197–204
56. Pages, G., Lenormand, P., L'Allemain, G., Chambard, J. C., Meloche, S., and Pouyssegur, J. (1993) *Proc. Natl. Acad. Sci. U. S. A.* **90**, 8319–8323
57. Sebolt-Leopold, J. S., and Herrera, R. (2004) *Nat. Rev. Cancer* **4**, 937–947
58. Sahai, E., and Marshall, C. J. (2002) *Nat. Rev. Cancer* **2**, 133–142
59. Bar-Sagi, D., and Hall, A. (2000) *Cell* **103**, 227–238
60. Jaffe, A. B., and Hall, A. (2005) *Annu. Rev. Cell Dev. Biol.* **21**, 247–269
61. Lin, M., and van Golen, K. L. (2004) *Breast Cancer Res. Treat.* **84**, 49–60
62. Fritz, G., Just, I., and Kaina, B. (1999) *Int. J. Cancer* **81**, 682–687
63. Qiu, R. G., Chen, J., Kirn, D., McCormick, F., and Symons, M. (1995) *Nature* **374**, 457–459
64. Peifer, M., and Polakis, P. (2000) *Science* **287**, 1606–1609
65. Jiang, W. G. (1996) *Br. J. Surg.* **83**, 437–446

IQGAP1 Stimulates Proliferation and Enhances Tumorigenesis of Human Breast Epithelial Cells

Lorraine Jadeski, Jennifer M. Mataraza, Ha-Won Jeong, Zhigang Li and David B. Sacks

J. Biol. Chem. 2008, 283:1008-1017.

doi: 10.1074/jbc.M708466200 originally published online November 2, 2007

Access the most updated version of this article at doi: [10.1074/jbc.M708466200](https://doi.org/10.1074/jbc.M708466200)

Alerts:

- [When this article is cited](#)
- [When a correction for this article is posted](#)

[Click here](#) to choose from all of JBC's e-mail alerts

This article cites 65 references, 23 of which can be accessed free at <http://www.jbc.org/content/283/2/1008.full.html#ref-list-1>